Catalysis Today 424 (2023) 113801

Contents lists available at ScienceDirect

Catalysis Today

journal homepage: www.elsevier.com/locate/cattod

# Beta zeolite as an efficient catalyst for the synthesis of diphenolic acid (DPA) from renewable levulinic acid

Gabriel Morales *, Juan A. Melero, Marta Paniagua, Clara López-Aguado, Nora Vidal

*Chemical and Environmental Engineering Group, Universidad Rey Juan Carlos, C/Tulipán s/n. Móstoles, 28933 Madrid, Spain*

ARTICLE INFO

*Keywords:*
Diphenolic acid
DPA
Levulinic acid
Sulfonic acid catalyst
Beta zeolite
Lignocellulosic biomass

ABSTRACT

The solvent-free production of diphenolic acid (DPA) from levulinic acid (LA) and phenol is studied using readily accessible commercial acid zeolites like Beta, ZSM-5 and USY. Acid zeolites are cost-effective catalysts, and they are herein benchmarked against the sulfonic acid resins Amberlyst-15 and Nafion®, and sulfonic acid-functionalized SBA-15 silicas. Beta zeolite with a moderate aluminum content (H-Beta 19, Si/Al=23) presents the best catalytic performance, owing to the right combination of the shape selectivity effect conferred by the BEA structure, and the adequate balance of acidity (Al content and speciation). The optimization of the reaction conditions is tackled by the response surface methodology using as optimization factors the temperature, the PhOH:LA molar ratio, and the catalyst loading. Thus, under the optimized reaction conditions (12 mmol LA, 140 °C, 0.30 g catalyst loading, PhOH:LA = 6:1 mol), over 70% yield to DPA with LA conversion around 77% is obtained after 72 h. Despite the catalyst shows a progressive activity decay in successive uses because of fouling, removal of the formed organic deposits by calcination in air allows restoring the starting catalytic performance.

## 1. Introduction

Assuring the renewability and sustainability of carbon-based resources is currently one of the priorities to minimize the associated environmental impacts, as well as to provide a solution to the eventual depletion of fossil resources. In this context, the center of attention is focused on biomass, as a resource for the production of chemicals and fuels alike [1–6]. During the last years, many processes have been proposed for the conversion of biomass, with some of them reaching an advanced development stage or even commercial deployment [2,7]. Lignocellulosic biomass is particularly interesting as a versatile raw material for C-based products, especially considering its worldwide abundancy and availability. Nevertheless, the industrial production of valuable chemicals and fuels from lignocellulose still requires of extensive efforts in designing, developing and intensifying cost-effective catalytic processes, according to the concept of biorefinery [8–15]. The chemical valorization of lignocellulose into high-quality fuels and chemicals typically follows an initial acid hydrolysis targeted to a selective production of platform molecules like levulinic acid, 5-hydroxymethyl furfural, or furfural [16–18]. Among them, levulinic acid (LA) was revealed as one of the top-10 most promising platform molecules derived from biomass by the U.S. Department of Energy [19], and it is widely considered as a key element in the developing lignocellulosic biorefining industry [20]. Indeed, several companies from different countries are already engineering industrial processes aiming at the large-scale production of levulinic acid as precursor for many other bioproducts (i.e., lactones, levulinate esters, amino-levulinic acid, valeric biofuels, bio-monomers, etc.) [21–23].

On the other hand, the development of environmentally friendly monomers based on biomass platform chemicals like LA is receiving growing attention [24]. In order to incorporate levulinic acid as a building unit into a polymer chain, it needs, however, to be first chemically converted to serve as a monomer [25–27]. Among the different approaches, LA can be easily cyclized via reactive distillation to obtain α-angelica lactone, which can be used as monomer in polymerizations. However, the formed polymers fail to reach an acceptable level of quality, and mixtures of α- and β-angelica lactones have been considered [28]. It is also possible to hydrogenate LA to 1,4-pentanediol (1,4-PDO), that can be subsequently used to produce polyesters, ideally in combination with bio-based diacids [29]. δ-amino-levulinic acid (DALA), obtained from LA by selective introduction of an amino group at the C5-position via bromination, has also shown the potential for the production of renewable polymers [30]. Finally, the condensation of LA with two molecules of phenol, which can be also derived from the lignin

* Corresponding author.
*E-mail address:* gabriel.morales@urjc.es (G. Morales).

https://doi.org/10.1016/j.cattod.2022.06.016
Received 28 February 2022; Received in revised form 20 May 2022; Accepted 11 June 2022
Available online 15 June 2022

fraction of lignocellulose, yields 4,4-bis-(4′-hydroxyphenyl)pentanoic acid, also known as diphenolic acid (DPA). DPA is proposed as a surrogate for bisphenol A, the primary raw material in epoxy resins and polycarbonates [31–33], widely used as chemical intermediate in paint formulations, decorative and protective surface coatings, additives for lubricating oil, plasticizers, surfactants, cosmetics, and textile industry [34,35]. Additionally, DPA bears several functional moieties rendering it amenable to further chemical modification, opening up new routes to much more functionalized materials and providing new sustainable opportunities for the chemical industry [36,37]. Therefore, in the long term and considering a favorable scenario of highly-available inexpensive LA, DPA appears as a viable alternative for the production of plastics [32].

The condensation of LA and phenol takes place via Friedel-Crafts hydroxyalkylation, leading to the corresponding *p,p′* and *o,p′* isomers (Scheme 1). The formation of phenol oligomers with LA has also been reported, leading to products different from DPA isomers that would not find use as Bisphenol A surrogates [38], thus having a negative impact on the overall selectivity towards DPA of the production process. While both monomers are of potential interest as intermediates in the polymer industry, *p,p′*-DPA isomer is the one proposed as a direct alternative to bisphenol-A. Traditionally, the condensation reaction for the synthesis of DPA has been investigated using strong Brønsted mineral acids such as $H_2SO_4$ and HCl [39]. The use of these acids is well known to suffer from problems concerning corrosiveness, difficulties in handling and separation from reaction media, as well as expensive downstream waste treatment [40]. As in many other acid catalysis applications, in the last decades such environmental and management concerns have prompted the development of solid acid catalysts to replace toxic and corrosive reagents.

In this way, the production of diphenolic acid has been investigated using mesoporous $H_3PW_{12}O_{40}$/silica composites prepared by direct sol-gel condensation [41–43]. In these studies, SBA-15 silica provided the best catalytic performance due to its highly accessible mesoporous structure, leading to TOFs over $1.5 \times 10^{-2}$ $s^{-1}$ (4:1 PhOH:LA molar ratio at 100ºC). Though the catalyst was rapidly deactivated, it could be regenerated via calcination. Sulfonated hyperbranched poly(arylene oxindole)s were also evaluated as catalyst in the condensation of phenol and LA, including the use of 1:1 molar ratio of thiols as promoting additives [38]. Over this somehow sophisticated catalytic system, LA conversion and DPA yield ca. 70% and 53%, respectively, were achieved (TOF $3.6 \times 10^{-4}$ $s^{-1}$). Although this water-soluble polymer can be recovered by ultrafiltration [44], the authors did not report about the recycling and stability of the prepared sulfonated hyperbranched poly (arylene oxindole), or about the recovery of the promoting thiols. As a way of comparison, in the same work by Van de Vyver et al., other solid acid catalysts such as Amberlyst-15, Nafion NR50 and neat $H_3PW_{12}O_{40}$ were also studied, but they displayed poorer performances. In a similar way, thiol-containing Brønsted acidic ionic liquids (BAILs) have been tested in the condensation of phenol and LA, offering a high yield of DPA (over 90 mol% after 48 h) with a maximum TOF of $2.34 \times 10^{-5}$ $s^{-1}$ [45]. A further advance was the use of a low-cost mineral acid ($H_2SO_4$) for the synthesis of such BAILs. Shen et al. reported the favorable results

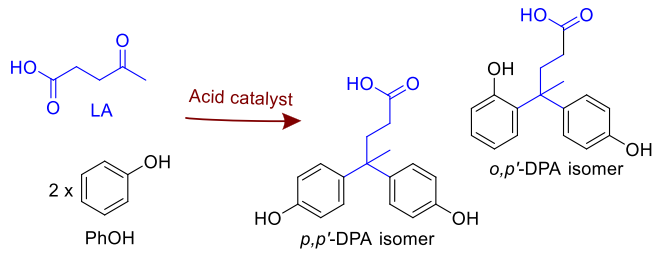


**Scheme 1.** Condensation of levulinic acid and two molecules of phenol catalysed by acids.

on the condensation of phenol and LA catalysed by [BSMim]$HSO_4$ ionic liquid by adding a catalytic amount of ethanethiol to improve the yield of DPA (reaching values over 90%) [42]. Favorable results were attributed to the special structure of the ionic liquids and the involvement of thiol additive. Moreover, BAILs could also catalyze the reaction of levulinate esters with phenol or the direct esterification of DPA to produce diphenolic esters. However, the authors did not report data on the stability and reusability of such methodology.

Despite the high conversion and yields to DPA so far obtained over the reported heterogeneous catalytic systems, underlying concerns regarding the high susceptibility to leaching as well as elevated costs still make necessary the development of more robust and inexpensive solid acid catalysts. In this work, the solvent-free production of diphenolic acid is studied using as catalysts readily accessible commercial acid zeolites like Beta, ZSM-5 and USY. Acid zeolites are well-known cost-effective catalysts with a proved history of success in large-scale industrial applications, mainly in oil refining and petro-chemistry. Various other acid catalysts, namely the sulfonic acid resins Amberlyst-15 and Nafion®, as well as sulfonic acid-functionalized SBA-15 silicas, are also benchmarked in the production of DPA from LA. The optimization of the reaction conditions is tackled by response surface methodology (RSM), using as optimization parameters the reaction temperature, the PhOH: LA molar ratio, and the catalyst loading. Furthermore, under the optimized reaction conditions, the reusability of the most efficient catalyst is analysed.

## 2. Experimental

### 2.1. Commercial catalysts and reactants

Zeolites were acquired from different suppliers: Beta 12.5 (CP 814E), Beta 19 (CP 814 C), and USY (CBV 712) from Zeolyst International, Beta 75 (CBZ 150) and n-ZSM-5 (CZP 90) from Clariant, and Beta 180 (45875) from Alfa Aesar. Acidic macroporous resin Amberlyst-15 was supplied by Sigma-Aldrich. Levulinic acid (Sigma-Aldrich, 98%) and phenol (Scharlau, Pharmpur® >99%) were used as reactants, whereas sulfolane (Sigma-Aldrich, 99%) was used as internal standard. Acetone (99.9%, Scharlau) and deuterated tetrahydrofuran ($C_4D_8O$, 99.5% D, Eurisotop) were used as analytical solvents for gas chromatography and $^1H$ NMR spectroscopy, respectively. Commercial diphenolic acid (4,4-bis(4-hydroxyphenyl)valeric acid, Sigma-Aldrich, 95%) was used as a reference for product identification and quantification.

### 2.2. Synthesis of sulfonic acid-modified SBA-15 mesoporous silicas

Propylsulfonic-acid functionalized mesostructured silica (Pr-$SO_3H$-SBA-15) was synthesized following the reported classical co-condensation procedure [46]. Thus, block-copolymer Pluronic P-123 ($EO_{20}PO_{70}EO_{20}$, Sigma-Aldrich) was used as surfactant template, tetraethylorthosilicate (TEOS, Sigma-Aldrich, 98%) as silica precursor, and (3-mercaptopropyl)trimethoxysilane (MPTMS, Sigma-Aldrich, 95%) as sulfur precursor. In a similar way, arenesulfonic-acid functionalized mesostructured silica (Ar-$SO_3H$-SBA-15) was prepared following a previously reported procedure [47]. In this case, 2-(4-chlorosulfonylphenyl)ethyltrimethoxysilane (CSPTMS, Abcr GmbH, 50% in $CH_2Cl_2$) was used as sulfur precursor. For both materials, the amount of S precursors (MPTMS and CSPTMS) was fixed to provide a theoretical loading of 10 mol% of sulfonic sites (based in total silicon content).

Nafion-SBA-15 was prepared by impregnating a solution of Nafion resin over a previously synthesised SBA-15 silica support [48]. The incorporation of the perfluorosulfonic Nafion resin was carried out by contacting the appropriate amount of Nafion alcoholic solution (Aldrich, Nafion resin at 5% in a mixture of lower aliphatic alcohols and water) with the powdered SBA-15 silica [49]. Theoretical resin loading was fixed at 15 wt%. The impregnation process was carried out at 60 ºC under vigorous stirring for 2 h. Alcoholic solvent was removed by

evaporation at room temperature for 24 h.

### 2.3. Catalysts characterization

The textural properties of the sulfonic acid-modified mesostructured silicas were determined by nitrogen adsorption-desorption isotherms recorded at − 196 °C (77 K) using a Micromeritics TriStar 3000 unit. In the case of zeolites, textural properties were calculated from argon adsorption-desorption isotherms recorded at − 186 °C (87 K), using an AutoSorb equipment (Quantachrome Instruments). Zeolites were previously degassed under vacuum at 273 ºC for 3 h. Contribution of micropores to surface and volume (in zeolites) was calculated by using the NL-DFT model assuming cylindrical pore geometry. Total surface area was obtained in both cases from the adsorption isotherms using the BET method, and total pore volume was extracted at approximately $P/P_o = 0.98$. Structural ordering was obtained by means of X-ray powder diffraction (XRD) patterns, acquired on a Philips X'Pert diffractometer using the Cu Kα line. Data were recorded from 0.6° to 5° (2θ) with a resolution of 0.02 ° for the mesoporous materials, and from 5° to 60° with a step size of 0.04 ° for zeolites. The number of sulfonic acid sites was potentiometrically assessed by titrating a suspension of 0.05 g of material in 15 g of 2 M NaCl (aq) with 0.01 M NaOH (aq). Sulfur content was determined by means of elemental analysis (Flash 2000 Organic Elemental Analyser, from Thermo Scientific). Organic content was evaluated through thermogravimetric analysis (SDT 2960 Simultaneous DSC-TGA, from TA Instruments) with an air flow-rate of 100 mL/min and a heating ramp of 5 ºC/min. In the case of zeolites, aluminum content was determined by Inductively-Coupled Plasma Optical Emission Spectroscopy (ICP-OES) using a Varian Vista AX apparatus. Likewise, solid-state $^{27}$Al MAS NMR spectra were recorded at room temperature on a Bruker Advance III/HD 400 spectrometer equipped with a 4 mm MAS probe operating at 9.4 T. Temperature-programmed desorption of ammonia ($NH_3$-TPD) was used to determine the total acid capacity of the zeolites in a Micromeritics Autochem 2910 (TPD/TPR) unit coupled to a TCD detector.

### 2.4. Catalytic tests

The reactions were carried out in ACE pressure glass reactors immersed in a silicone oil bath under temperature control and vigorous continuous magnetic stirring. At the given reaction time, tube reactor is removed from the bath and the reaction media is processed for analysis. A typical composition of the reaction mixture for a 4:1 PhOH:LA experiment is 1.38 g (12 mmol) of levulinic acid, 4.5 g (48 mmol) of phenol, 0.1 g of sulfolane as internal standard, and the respective mass of catalyst. It must be noted that while both phenol and levulinic acid can have a biomass origin, the ones used in this study are both pure commercial materials. In the set of experiments for catalysts screening, reaction time and temperature were fixed at 24 h and 120 ºC, respectively, adding 0.225 g of catalyst. In the experiments related to the optimization of reaction conditions, the reaction variables and ranges investigated were: temperature (100–140 ºC), molar ratio PhOH:LA (2:1–6:1), catalyst loading (0.15–0.30 g), time (0–72 h). Thereafter, under the optimized reaction conditions, a reusability study was carried out.

### 2.5. Reaction analysis

Reaction samples were analysed using gas chromatography (GC), and nuclear magnetic resonance (NMR) spectroscopy. LA conversion was analysed by GC, after first diluting the reaction mixture with acetone, using a Varian 3900 gas chromatograph equipped with an Agilent CP-WAX 52 CB column (30 m x 0.25 mm, DF = 0.25 μm) and a flame ionization detector (FID). LA quantification was based on a calibration of the GC analysis unit with a standard stock solution of pure commercially available chemical using sulfolane as the internal standard. On the other hand, DPA was quantified by means of NMR based on the spectrum of commercial diphenolic acid. Thus, a 0.2 mL aliquot was taken from the reaction medium (before diluting with acetone for the GC analysis), and subsequently dissolved in deuterated tetrahydrofuran and filtered to remove any catalyst particles. $^1$H NMR analysis was then performed in a Varian Mercury Plus spectrometer operating at 400 MHz, allowing for the quantification of DPA in the reaction mixture, as well as for an approximate distribution of both DPA isomers, *o,p′*- and *p,p′*-isomers (Scheme 1). For the quantification of the proportion of both isomers, the $^1$H NMR signal centred at 1.55 ppm has been assigned to the free methyl group in the *p,p′*-isomer; whereas the signal centred at 1.50 ppm has been ascribed to the $CH_3$ moiety in the *o, p′*-isomer. Thus, catalytic results are shown in terms of conversion of levulinic acid ($X_{LA}$), yield to DPA ($Y_{DPA}$), selectivity to DPA ($S_{DPA}$), and specific productivity of DPA per acid site ($SP_{DPA}$) (Eqs. 1–4).

$$X_{LA} = \frac{Reacted\ \ mol\ \ of\ \ LA}{Initial\ \ mol\ \ of\ \ LA} \times 100 \quad (1)$$

$$Y_{DPA} = \frac{Formed\ \ mol\ \ of\ \ DPA}{Initial\ \ mol\ \ of\ \ LA} \times 100 \quad (2)$$

$$S_{DPA} = \frac{Y_{DPA}}{X_{LA}} \times 100 \quad (3)$$

$$SP_{DPA}\ \ \left(\frac{mol\ \ DPA}{mol\ \ H^+}\right) = \frac{Formed\ \ mol\ \ of\ \ DPA}{Acid\ \ capacity\ \ \left(\frac{mol\ \ H^+}{g}\right) \cdot Catalyst\ \ mass\ \ (g)} \quad (4)$$

## 3. Results and discussion

### 3.1. Screening of acid catalysts for the synthesis of DPA

In this type of heterogeneous acid catalysis, the nature, number and distribution of acid sites display a strong influence on the catalytic performance, i.e. in the conversion, yield and selectivity to DPA. Therefore, different acid solids have been benchmarked in reaction, including sulfonic-acid based materials (Brønsted acid catalysts) and commercial acid zeolites (catalysts showing both Brønsted and Lewis acidity). The most relevant physicochemical properties of the different catalysts tested in this work are presented in Tables 1 and 2.

Table 1 summarizes the properties of the sulfonic acid-based materials, including the synthesised mesostructured materials and the cationic-exchange acidic resin Amberlyst-15. In the case of the propyl- and arene-$SO_3H$ SBA-15 mesoporous silicas, data from XRD and nitrogen adsorption isotherms (not shown) evidence high mesoscopic ordering (2D-hexagonal *p6mm* symmetry) and high surface areas along with narrow pore size distributions around 8–9 nm, typical of SBA-15 structures. Both materials were synthesised to incorporate 10% of the respective sulfur precursor, corresponding to approximately 1 meq S/g.

**Table 1**
Physicochemical, textural and acidity-related properties for sulfonic acid-based catalysts.

| Catalyst | Acid capacity[a] (meq $H^+$/g) | $S^b_{BET}$ ($m^2$/g) | $D^c_p$ (Å) | $V^d_p$ ($cm^3$/g) | $SO_3H$ groups density[e] (μeq $H^+/m^2$) |
|---|---|---|---|---|---|
| Ar-$SO_3H$-SBA-15 | 1.09 | 751 | 87 | 0.88 | 1.4 |
| Pr-$SO_3H$-SBA-15 | 1.05 | 772 | 88 | 1.29 | 1.4 |
| Amberlyst-15 | ≥ 4.70 | 45 | 300 | 0.40 | 104 |
| Nafion-SBA-15 | 0.10 | 496 | 66 | 0.78 | 0.2 |

[a] Acid capacity determined by acid-base titration. [b] Surface area calculated by the BET method. [c] Mean pore size from the adsorption branch of the $N_2$ isotherm. [d] Total pore volume at $P/P_o \approx 0.98$. [e] Acid sites density defined as the ratio between acid capacity from acid-base titration and the BET surface area.

**Table 2**
Physicochemical, textural and acidity-related properties for acid zeolites.

| Catalyst | Aluminum content | | Textural properties | | | | | | Acid Properties | |
|---|---|---|---|---|---|---|---|---|---|---|
| | Si/Al[a] (mol) | Tet. Al[b] (%) | $S^c_{BET}$ ($m^2/g$) | $S^d_{EXT}$ ($m^2/g$) | $S^e_{\mu}$ ($m^2/g$) | $S_{\mu}/S^f_{BET}$ | $V^g_p$ ($cm^3/g$) | $D^h_p$ (Å) | $NH_3$-TPD[i] (meq $H^+/g$) | Density[j] (μeq $H^+/m^2$) |
| n-ZSM5 | 42 | 98 | 488 | 196 | 291 | 0.60 | 0.49 | 5.1–5.6 | 0.33 | 0.68 |
| H-USY | 8 | 48 | 884 | 136 | 748 | 0.85 | 0.54 | 7.4 | 0.88 | 1.00 |
| H-Beta 12.5 | 16 | 78 | 600 | 196 | 404 | 0.67 | 0.90 | 5.6–7.7 | 0.65 | 1.08 |

[a] Si/Al molar ratio as measured by ICP-OES. [b] Tetrahedral Al as calculated by solid-state $^{27}$Al MAS NMR. [c] Surface area calculated by the BET method. [d] External surface area. [e] Micropores surface area. [f] Micropores surface area to BET surface area ratio. [g] Total pore volume at $P/P_o \approx 0.98$. [h] Pore size range corresponding to each crystalline structure. [i] Total acid capacity as determined by $NH_3$-TPD. [j] Acid sites density is defined as the ratio between acid capacity from $NH_3$-TPD and BET surface area.

This value is in good agreement with the acid capacity as determined by acid-base titration (Table 1), so a high S incorporation degree in the form of sulfonic acid is inferred. Overall, these materials display open structures with high surface development and a good distribution of catalytic acid sites, leading to a low density thereof (1.4 μeq $H^+/m^2$, Table 1), which renders them as excellent candidates to be tested in reaction. Table 1 also includes the physicochemical properties as provided by the supplier corresponding to the commercial sulfonic acid resin, Amberlyst-15, as well as the properties from the hybrid material Nafion®/SBA-15 herein prepared. Amberlyst-15 shows a very high acid capacity on a non-structured polymer matrix showing low specific surface. Thus, this material has an acid density two orders of magnitude higher than $SO_3H$-SBA-15 catalysts. Finally, the composite comprising perfluorosulfonic Nafion resin over SBA-15 retains in a large extent the good textural properties of the mesoporous support while incorporating on it highly dispersed Nafion resin (15 wt%) [49]. This composite shows the lowest acid capacity and acid density because of the low acid loading of the resin itself. However, the perfluoro environment surrounding the sulfonic acid sites provides them with the highest acid strength.

On the other hand, Table 2 includes the most relevant physicochemical properties of the selected zeolites. Acid properties of zeolites depend particularly on the framework type and aluminum content and speciation. Hence, in the present work three commercial zeolites with different crystalline structures (MFI for n-ZSM5, FAU for H-USY, BEA for H-Beta 12.5) with varying Si/Al ratio have been chosen for evaluation. The determination of actual Al content by means of ICP-OES confirmed a variability in the Si/Al ratio, as intended, ranging from 8 to 42. On the other hand, textural properties obtained from the Ar adsorption-desorption isotherms at − 186 °C (not shown), evidence the presence of a high total BET surface area and high micropores surface area in every material, with mean pore sizes in the corresponding microporous range (5–8 Å). Additionally, pore volumes range between 0.49 and 0.90 $cm^3/g$. The highest value, corresponding to H-Beta 12.5 is attributed to a contribution of inter-particle argon adsorption. Regarding the acid properties, the highest acid capacity, as determined by $NH_3$-TPD, corresponds to H-USY zeolite, which is in agreement with its higher Al content. However, in this case a great proportion of the aluminum is in extra-framework octahedral configuration (as determined by $^{27}$Al NMR). In terms of acid surface density, H-Beta 12.5 leads to the highest value, in this case with a larger proportion of intra-framework Al (78%). In conclusion, the microporous structure, together with the ratio $S_{\mu}/S_{ext}$ and the concentration and speciation of Al species, are all parameters expected to influence on the catalytic performance. A more detailed discussion on the acid properties of these specific materials is available elsewhere [50].

Fig. 1 shows the catalytic results of the materials evaluated in the acid-catalysed solvent-free condensation of levulinic acid and phenol, in terms of conversion of levulinic acid ($X_{LA}$), and yield to diphenolic acid ($Y_{DPA}$). Reaction conditions for this catalysts benchmarking were selected based in previous studies from literature [42,51].

Regarding sulfonic acid-based catalysts (left), Amberlyst-15 displayed the highest conversion (63.2%), though the yield to DPA is only

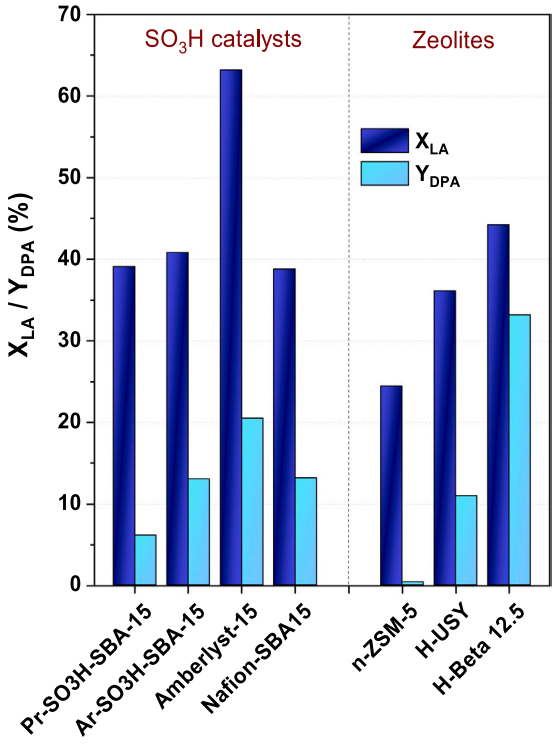


**Fig. 1.** Conversion of LA and yield to DPA over the different solid acid catalysts evaluated. Reaction conditions: 120 °C, 0.225 g catalyst loading, 24 h, Phenol: LA = 4:1 (mol).

20.5%, indicating low selectivity of this kind of catalyst. On the other hand, the synthesized perfluoro-, propyl- and arene-$SO_3H$-SBA-15 catalysts, provided all a similar behavior in terms of conversion of levulinic acid. Regarding the yield and productivity of DPA, and considering the different nature of the sulfonic acid sites incorporated on these SBA-15 silicas, it is possible to observe a positive trend related to the increase of acid strength: fluor-$SO_3H$ (Nafion) > arene-$SO_3H$ > propyl-$SO_3H$. Still, the selectivity to DPA is very low in each case, as observed for Amberlyst-15. This can be attributed to the presence of undesired side reaction of levulinic acid in the presence of such strong Brønsted acid catalysts, which apparently occurs regardless of the surface acid sites concentration. Additionally, no apparent effect of the SBA-15 mesoporous framework is observed. Therefore, these materials are discarded for further studies.

On the other hand, among the commercial zeolites (Fig. 1 right), n-ZSM5 zeolite is able to convert LA but does not produce DPA. We attribute such an effect to the limited pore size of MFI structure, which largely hinders the formation of the bulky condensation product coming from the combination of 2 molecules of PhOH and 1 of LA, even in the positions corresponding to external surface area. The USY zeolite in turn

behaves in a similar way to sulfonic materials, with the same low selectivity. In this case, the larger pore size (with respect to n-ZSM5), and the high acid capacity and strength of H-USY resemble those of $SO_3H$-based SBA-15 catalysts, so that the same type of undesired side reactions most likely take place over this catalyst. Finally, H-Beta 12.5 zeolite displays the best performance in the catalyst screening, both in terms of DPA yield (33.1%) and selectivity (75%). This is attributed to a right combination of pore size and structure (BEA framework), which would be especially tailored for the molecules involved in this transformation, together with the appropriate type and moderate strength of acid sites.

To complete the catalysts screening, the respective production of the two DPA isomers (Scheme 1) was also assessed. It must be noted that, while both isomers are of potential interest as intermediates in the polymer industry, the most linear one, *p,p′*-DPA isomer, is the one proposed as a direct alternative to Bisphenol-A, so that its market value would be potentially higher. Taking this into account, the proportion of both isomers over the different catalysts has also been analysed. Fig. 2 depicts the DPA isomers distribution in the above-discussed catalysts benchmarking (values obtained from the $^1$H NMR analysis of reaction samples). As shown, there is a clearly different behavior between sulfonic materials and zeolites: the former preferentially give rise to *o,p′*-DPA, regardless the presence of SBA-15 structured support, while the latter provide higher ratio of *p,p′*-DPA. Noticeably, H-Beta 12.5 catalyst results in the highest proportion of *p,p′*-DPA, which would be in line with a remarkable shape selectivity effect associated to its particular microcrystalline structure, as compared to the other zeolites.

### 3.2. Effect of the Si/Al ratio in Beta zeolites

As previously discussed, beta zeolite has displayed the best catalytic performance in the solvent-free production of DPA, not only from the point of view of yield and selectivity to DPA, but also considering the preferential production of the most preferred isomer. Thus, we extended the study to incorporate other commercially available beta zeolites with varying Al content.

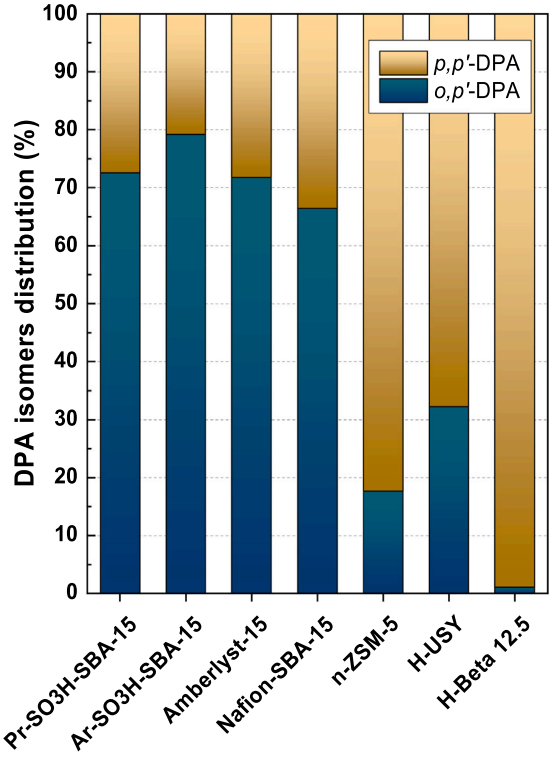


**Fig. 2.** DPA isomers distribution over the different solid acid catalysts. Reaction conditions: 120 °C, 0.225 g catalyst loading, 24 h, Phenol:LA = 4:1 (mol).

Table 3 incorporates highlighted physicochemical properties corresponding to the four beta zeolites herein evaluated. As shown, actual Si/Al ratios (slightly different to those proposed in the commercial specs) allow for testing a series of beta materials with different Si/Al ratio in the reaction of DPA production. Indeed, Si/Al ratio is the key parameter affecting the acid properties of this type of materials, determining not only the amount and concentration of acid sites (as shown in Table 3, from $NH_3$-TPD) but also their nature (Brønsted and Lewis) and strength. For more details, see our recent work on these specific materials applied to the dimerization of levulinic acid for the production of jet-fuel precursors, where the use of base probe molecules such as $CD_3CN$ and pyridine in DRIFT spectroscopy allowed for a precise discrimination of the acid properties [50]. Regarding the textural properties, all the beta zeolites display high surface area, mainly in the microporous region ($S_\mu/S_{BET} > 0.67$). The differences can be attributed to the different synthesis methods applied by the manufacturers, though they are not deemed significant for the following discussion of reaction results.

Fig. 3 summarizes the catalytic performance of the four samples of beta zeolites in the condensation of levulinic acid and phenol to produce diphenolic acid, in terms of LA conversion and yield to DPA (Fig. 3A), as well as in terms of specific productivity of DPA per acid site (Fig. 3B). Reaction conditions are the same used in the previous screening of catalysts to facilitate the comparison.

As shown in Fig. 3, the catalytic performance of the different beta zeolites reflects a marked influence of the aluminium content (i.e., the Si/Al ratio). The four materials share the high activity and selectivity to DPA previously discussed in the catalysts screening, but with interesting differences. Thus, H-Beta 75 (SiAl = 103) results in the highest LA conversion and yield to DPA. Likewise, when analysing the specific productivity of DPA per acid site (at 24 h of reaction time), the highest value corresponds to H-Beta 75 (115 $mol_{DPA}/mol_{H+}$). This material has a high proportion of tetrahedral Al (96%, Table 3) together with a low surface acid density (0.37 $\mu eqH^+/m^2$), indicating the presence of isolated strong Al acid sites in a purely silica microporous environment. This appears as the right combination to drive the reaction of DPA production (mainly the *p,p′* isomer) in an efficient way. However, from the point of view of biomass efficient utilization, together with a desirable reduction of the downstream separation necessities, we consider that the selectivity to DPA should have also a leading role in establishing the catalyst choice. In this sense, Fig. 4 depicts the variation of DPA selectivity ($S_{DPA}$) as a function of the Si/Al ratio in the series of beta zeolites. As shown, there is a maximum in the selectivity in an intermediate Si/Al window. Indeed, the most selective catalyst is the zeolite H-Beta 19, reaching a value of 84.3%, while still keeping high $X_{LA}$ and $Y_{DPA}$ (Fig. 3A).

In a recent work, we applied DRIFT analysis of adsorbed pyridine and deuterated acetonitrile molecules to the same series of Beta zeolites, allowing not only for distinguishing between Brønsted and Lewis acid sites, but also sorting them in terms of acid strength in a semi-quantitative manner [50]. A decreasing trend on the Brønsted/Lewis (B/L) acid sites ratio, as determined by pyridine adsorption, when decreasing the Al content was observed, showing a maximum B/L= 1.95 for H-Beta 19. Likewise, DRIFT experiments of adsorbed $CD_3CN$ allowed differentiating the relative contribution of Brønsted and Lewis acid sites in terms of acid strength. In this case, zeolite H-Beta 19 showed the presence of both strong Brønsted and strong Lewis acid sites, with a ratio $B_S/L_S$ around 2.0 [50]. Thus, this zeolite has an optimum B/L acid sites ratio and the adequate $B_S/L_S$ acid sites ratio to yield the best catalytic performance in terms of combined activity and selectivity in the production of DPA from LA.

On the other hand, taking into account the textural properties of the Beta zeolites, it seems that an intermediate $S_\mu/S_{BET}$ surface areas ratio (Table 3) also contributes to achieve high selectivity to DPA. In this way, zeolites H-Beta 19 and H-Beta 75 (displayng values of 0.83 and 0.74 for the $S_\mu/S_{BET}$ ratio) lead to the highest selectivities.

**Table 3**
Physicochemical, textural and acidity-related properties corresponding to commercial Beta zeolites with varying Si/Al ratio.

| Catalyst | Aluminum content | | Textural properties | | | | | | Acid Properties | |
|---|---|---|---|---|---|---|---|---|---|---|
| | Si/Al[a] (mol) | Tet. Al[b] (%) | $S_{BET}^{c}$ ($m^2/g$) | $S_{EXT}^{d}$ ($m^2/g$) | $S_{\mu}^{e}$ ($m^2/g$) | $S_{\mu}/S_{BET}^{f}$ | $V_{p}^{g}$ ($cm^3/g$) | $D_{p}^{h}$ (Å) | $NH_3$-TPD[i] (meq $H^+/g$) | Density[j] (μeq $H^+/m^2$) |
| H-Beta 12.5 | 16 | 78 | 600 | 196 | 404 | 0.67 | 0.90 | 5.6–7.7 | 0.65 | 1.08 |
| H-Beta 19 | 23 | 59 | 726 | 126 | 600 | 0.83 | 0.44 | 5.6–7.7 | 0.57 | 0.79 |
| H-Beta 75 | 103 | 96 | 573 | 151 | 422 | 0.74 | 0.57 | 5.6–7.7 | 0.21 | 0.37 |
| H-Beta 180 | 122 | 96 | 750 | 91 | 659 | 0.88 | 0.44 | 5.6–7.7 | 0.23 | 0.31 |

[a] Si/Al molar ratio as measured by ICP-OES. [b] Tetrahedral Al as calculated by solid-state $^{27}$Al MAS NMR. [c] Surface area calculated by the BET method. [d] External surface area. [e] Micropores surface area. [f] Micropores surface area to BET surface area ratio. [g] Total pore volume at $P/P_o \approx 0.98$. [h] Pore size range corresponding to each crystalline structure. [i] Total acid capacity as determined by $NH_3$-TPD. [j] Acid sites density is defined as the ratio between acid capacity from $NH_3$-TPD and BET surface area.

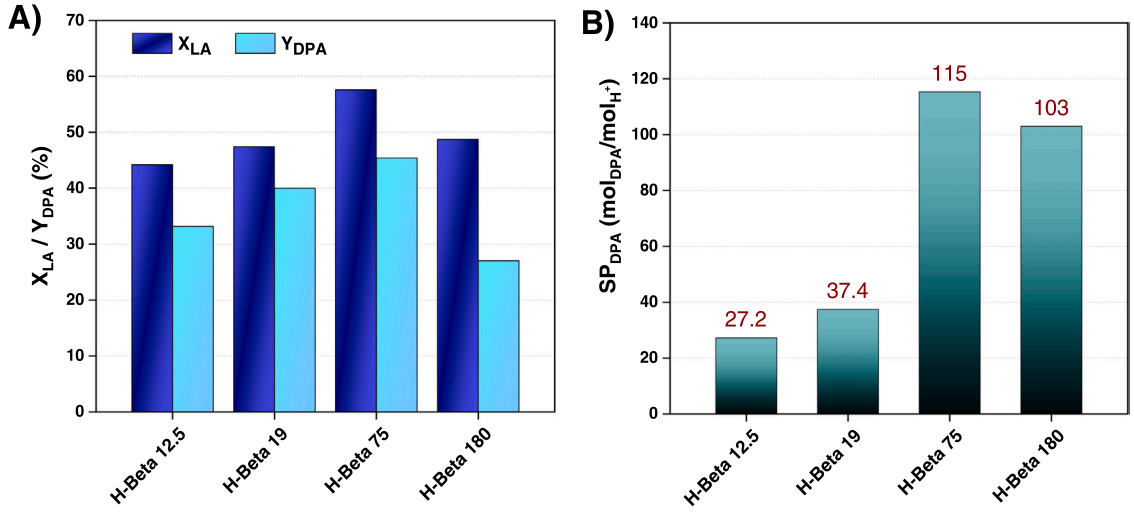


**Fig. 3.** A) Conversion of LA ($X_{LA}$) and yield to DPA ($Y_{DPA}$); and B) Specific Productivity of DPA per acid site ($SP_{DPA}$) in the solvent-free condensation of levulinic acid and phenol over beta zeolites with varying Si/Al ratio. Reaction conditions: 120 °C, 0.225 g catalyst loading, 24 h, Phenol:LA = 4:1 (mol).

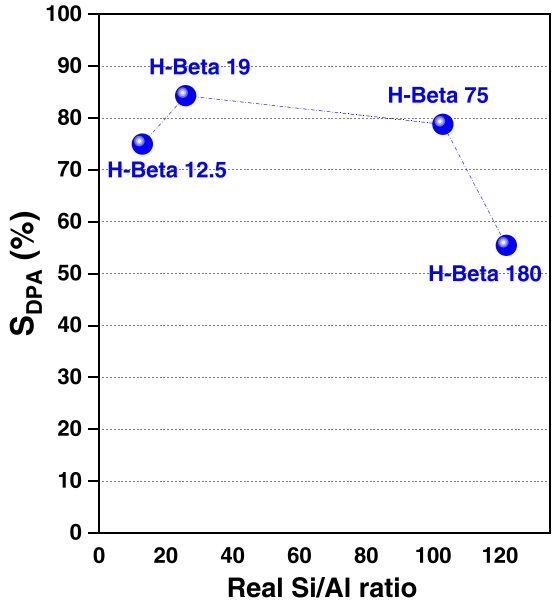


**Fig. 4.** Selectivity to DPA as a function of Si/Al ratio in beta zeolites. Reaction conditions: 120 °C, 0.225 g catalyst loading, 24 h, Phenol:LA = 4:1 (mol).

### 3.3. Statistical analysis and optimization of reaction conditions

Further optimization of the reaction conditions was explored for the selected catalyst, that is, H-Beta 19. The effect of the main operating variables (temperature, catalyst loading and Phenol:LA molar ratio) on the production of DPA was studied. The objective was to optimize the conversion of biomass-derived levulinic acid in the most selective way, in order to achieve high biomass efficiency use. For doing so, surface response methodology by means of experimental design was applied, leading to statistically significant mathematical models representing the behavior of the catalyst in the reaction system. The following operation windows were explored for optimization: temperature 100–140 °C; catalyst loading 0.15–0.30 g; Phenol:LA mol ratio 2:1–6:1, thus consisting of an analysis of three factors at three levels. Reaction time was fixed at 4 h for all the experiments, avoiding saturation at the highest conversions for a proper analysis of the catalytic data. The full-factorial design showing the coded and real values of the three factors analysed for each experiment (reaction variables) and their respective experimental observed responses (LA conversion and DPA yield) are listed in Table 4. The experiment corresponding to the central point of the design (0,0,0) was replicated four times in order to assess the experimental reproducibility of the results, as well as to quantify the experimental error. Noteworthy, to minimize interferences due to systematic trends in the manipulation and operation of the experimental and analytical setups, the order of the experiments was randomized. Assuming a second-order polynomial model applied to the experimental data matrix, equations (5) and (6) were obtained by multiple regression. These statistical models have been obtained from encoded levels of the factors, thus providing the actual influence of each reaction variable on the

**Table 4**
Full factorial design matrix of three variables at three levels along with the observed responses. Solvent-free condensation of levulinic acid and phenol into DPA over H-Beta-19.[a].

| Run# | Real Factors | | | Coded Factors | | | Observed Responses | |
|---|---|---|---|---|---|---|---|---|
| | T (ºC) | Cat. (g) | PhOH:LA (mol) | $I_T$ | $I_C$ | $I_R$ | $X_{LA}$ (%) | $Y_{DPA}$ (%) |
| 1 | 100 | 0.15 | 2 | -1 | -1 | -1 | 4.5 | 3.6 |
| 2 | 100 | 0.15 | 4 | -1 | -1 | 0 | 8.9 | 5.0 |
| 3 | 100 | 0.15 | 6 | -1 | -1 | +1 | 13.7 | 6.1 |
| 4 | 100 | 0.225 | 2 | -1 | 0 | -1 | 8.6 | 6.0 |
| 5 | 100 | 0.225 | 4 | -1 | 0 | 0 | 8.0 | 5.8 |
| 6 | 100 | 0.225 | 6 | -1 | 0 | +1 | 15.6 | 12.6 |
| 7 | 100 | 0.3 | 2 | -1 | +1 | -1 | 6.0 | 5.8 |
| 8 | 100 | 0.3 | 4 | -1 | +1 | 0 | 8.2 | 6.9 |
| 9 | 100 | 0.3 | 6 | -1 | +1 | +1 | 18.2 | 8.7 |
| 10 | 120 | 0.15 | 2 | 0 | -1 | -1 | 15.9 | 12.3 |
| 11 | 120 | 0.15 | 4 | 0 | -1 | 0 | 17.7 | 11.1 |
| 12 | 120 | 0.15 | 6 | 0 | -1 | +1 | 22.8 | 16.6 |
| 13 | 120 | 0.225 | 2 | 0 | 0 | -1 | 21.1 | 13.6 |
| 14 | 120 | 0.225 | 4 | 0 | 0 | 0 | 32.8 | 24.2 |
| 15 | 120 | 0.225 | 4 | 0 | 0 | 0 | 31.0 | 23.7 |
| 16 | 120 | 0.225 | 4 | 0 | 0 | 0 | 30.0 | 22.5 |
| 17 | 120 | 0.225 | 4 | 0 | 0 | 0 | 29.5 | 23.5 |
| 18 | 120 | 0.225 | 6 | 0 | 0 | +1 | 30.3 | 22.0 |
| 19 | 120 | 0.3 | 2 | 0 | +1 | -1 | 18.6 | 12.6 |
| 20 | 120 | 0.3 | 4 | 0 | +1 | 0 | 22.6 | 17.5 |
| 21 | 120 | 0.3 | 6 | 0 | +1 | 1 | 30.1 | 27.2 |
| 22 | 140 | 0.15 | 2 | +1 | -1 | -1 | 32.4 | 22.3 |
| 23 | 140 | 0.15 | 4 | +1 | -1 | 0 | 41.8 | 26.5 |
| 24 | 140 | 0.15 | 6 | +1 | -1 | 1 | 39.3 | 29.0 |
| 25 | 140 | 0.225 | 2 | +1 | 0 | -1 | 44.0 | 38.4 |
| 26 | 140 | 0.225 | 4 | +1 | 0 | 0 | 44.9 | 38.2 |
| 27 | 140 | 0.225 | 6 | +1 | 0 | 1 | 48.4 | 44.1 |
| 28 | 140 | 0.3 | 2 | +1 | +1 | -1 | 42.9 | 36.1 |
| 29 | 140 | 0.3 | 4 | +1 | +1 | 0 | 58.2 | 43.8 |
| 30 | 140 | 0.3 | 6 | +1 | +1 | +1 | 58.4 | 45.7 |

[a] Common reaction conditions: LA, 12 mmol, reaction time, 4 h. Note: T: temperature; C: catalyst loading; R: Phenol:LA molar ratio; I, coded value; $X_{LA}$, conversion of levulinic acid; $Y_{DPA}$, yield to diphenolic acid.

selected responses. Fig. 5 plots the resultant response surfaces and contour plots for $X_{LA}$ and $Y_{DPA}$, representing the combined effect of catalysts loading and reactants molar ratio at the three temperature levels, in order to provide a rapid and visual interpretation of the equations.

$$XLA = 56{\cdot}8367 - 1{\cdot}7010\bullet IT + 17{\cdot}2556\bullet IC + 3{\cdot}93667\bullet IR + 0.0087\bullet IT2 + 2{\cdot}3028{\cdot}IT{\cdot}IC - 0.0015{\cdot}IT{\cdot}IR - 625{\cdot}556{\cdot}IC2 + 9{\cdot}3778{\cdot}IC{\cdot}IR - 0.4434{\cdot}IR2 \quad (r2{=}0{\cdot}9624) \tag{5}$$

$$Y_{DPA} = 45{\cdot}6817 - 1{\cdot}5792\bullet I_T + 158{\cdot}122\bullet I_C + 0.3025\bullet I_R + 0.0072\bullet I_T^2 + 2{\cdot}2889{\cdot}I_T{\cdot}I_C - 0.0167{\cdot}I_T{\cdot}I_R - 901{\cdot}111{\cdot}I_C^2 + 6{\cdot}4889{\cdot}I_C{\cdot}I_R - 0.2655{\cdot}I_R^2 (r^2{=}0{\cdot}9543) \tag{6}$$

To validate the use of the models for making predictive analyses, the regression error was evaluated. Fitting goodness can be inferred from the high value recorded for the regression coefficients ($r^2$). Both of them are $> 0.95$, indicating a high correlation between the experimentally observed results and the predicted values. Additionally, the reproducibility of the experimental and analytical setups is elevated, as evidenced by the arithmetical averages and standard deviations calculated from the central-point replicas (runs 14–17, Table 4): LA conversion (30.8 ± 1.5%); yield to DPA (23.5 ± 0.7%). In this way, the reduced value of the standard deviations (≤ 1.5%) indicates that the experimental error is small.

An analysis of variance (ANOVA) was then applied to the experimental matrix of data to validate the significance of each parameter on the responses, using the total error criteria at 95.0% confidence level to obtain the respective P-values. Fig. 6 (left) shows the standardized Pareto charts for both responses, LA conversion and yield to DPA, allowing to easily identifying the most influential factors, as well as their statistical significance. As shown, the linear terms of the model ($I_T$, $I_C$, $I_R$) are the most important factors in both cases. The three of them has a positive effect on both responses, meaning that an enhancement of either temperature, catalyst loading or PhOH:LA molar ratio yields an increase in $X_{LA}$ and $Y_{DPA}$. However, it must be noted that the most influential parameter by large is the temperature. Additionally, no cross interaction between them is observed (at least in the range of values analysed), as evidenced by the major effects Charts represented in Fig. 6-right. Additionally, the quadratic terms of the model are of low significance, emphasising a negative contribution of the quadratic effect of catalyst loading ($I_C^2$), especially for the yield to DPA. This means that an increase of catalyst loading does not produce a constant rise in $X_{LA}$ and $Y_{DPA}$, because of the significant curvature effect observed at high values of this variable (Fig. 6-right), which can be explained in terms of the appearance of mass transfer hindrances at high solid catalyst concentration. In conclusion, the models show a rather linear behaviour and predict a low interaction among the reaction factors.

Fig. 5, including the respective response surfaces and contour plots of equations (5) and (6), represents in a clearly visual way the above-

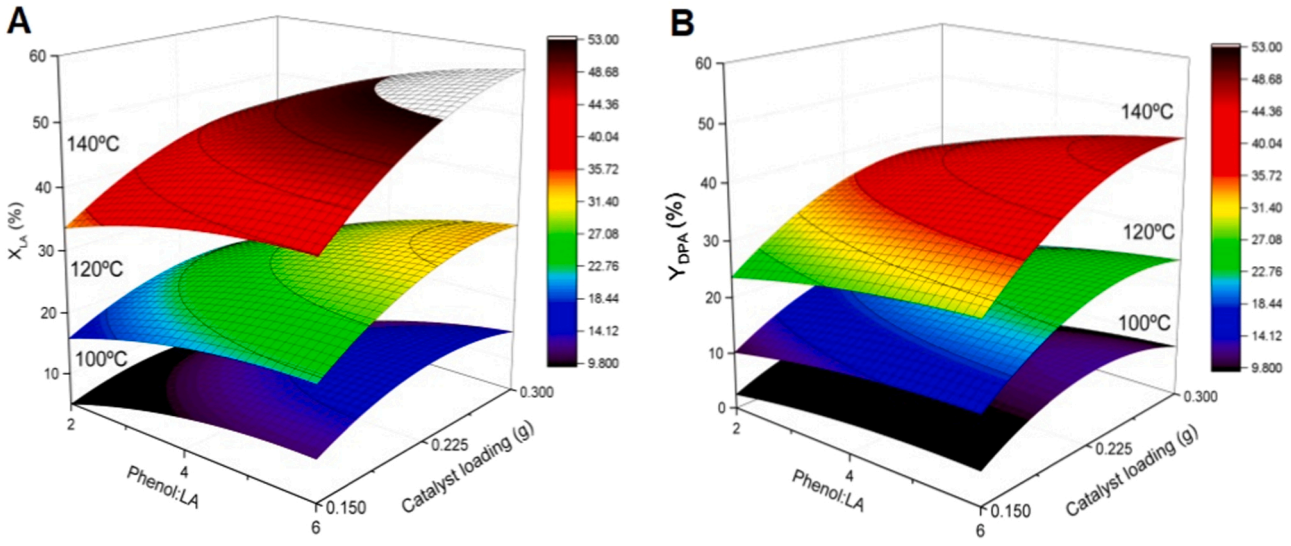


**Fig. 5.** Response surfaces and contour plots for the conversion of levulinic acid (A), and the yield to diphenolic acid (B) over H-Beta-19 catalyst. Reaction time: 4 h.

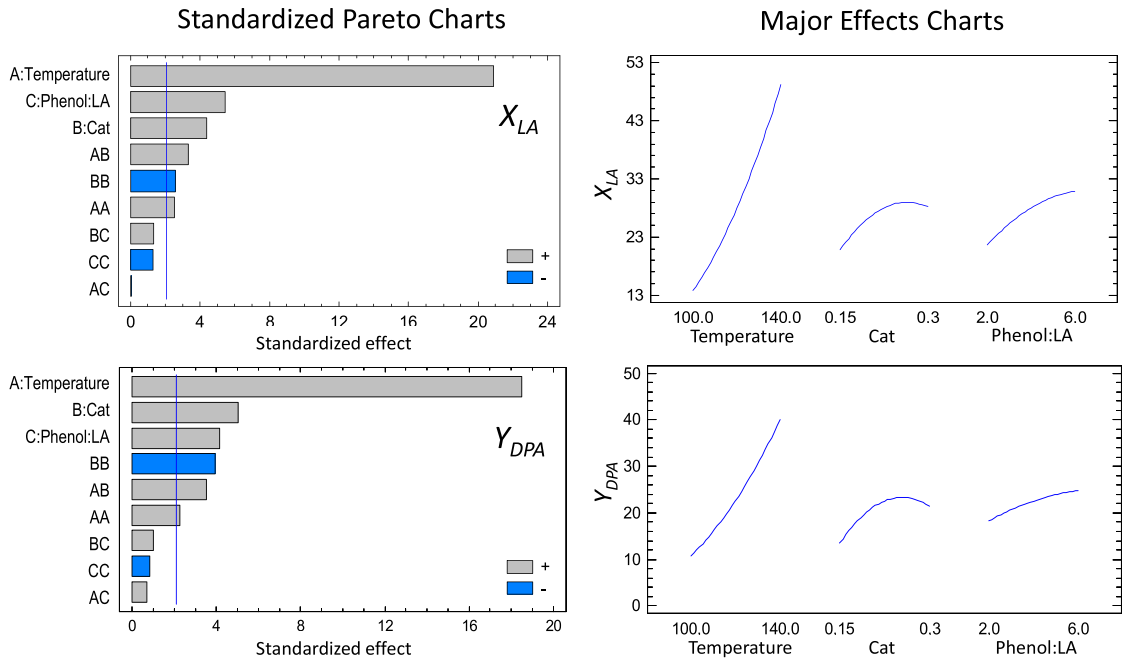


**Fig. 6.** Standardized Pareto charts (left) and Major Effects Charts (right) for LA conversion and yield to DPA.

mentioned effects as well as the lack of interactions among the three factors. Thus, the gradual increase of both $X_{LA}$ and $Y_{DPA}$ insofar as any of the factor increases is easily appreciated. Therefore, the optimal values under the range of study would be the highest temperature (140 °C), catalyst loading (0.3 g) and Phenol:LA molar ratio (6:1), corresponding to the run #30 (+1,+1,+1) of the experimental design. Under such conditions, LA conversion predicted by the model (Eq. 5) is 57.0% whereas the experimental result is 58.4%, in fair agreement with the model prediction. In the case of yield to DPA, the model (Eq. 6) provides a maximum predicted value of 46.5%, in good agreement with the experimental value attained under those specific reaction conditions (45.7%). Noteworthy, the selectivity to DPA at the optimized reaction conditions keeps being very high, 78.3%.

Since the temperature is the most influential parameter, and the selected optimum level of temperature coincides with the highest value in the experimental range, additional experiments were performed at higher temperatures (keeping constant the optimal PhOH:LA molar ratio and catalyst loading). Thus, two additional catalytic runs carried out at 160 °C and 180 °C led to slightly higher yields to DPA as compared to the result at 140 °C (50.3% and 46.7%, respectively), but at the expense of reducing the selectivity to DPA (70.7% and 67.6%, respectively). This indicates that the undesired side-reactions are favoured at higher temperatures. Therefore, the conditions optimized by the experimental design methodology are deemed as optimal to maximize the production of diphenolic acid from LA, while limiting the promotion of undesired side-reactions to reach the highest selectivity to DPA.

Then, under the optimized reaction conditions from the design of experiments, the effect of reaction time was assessed. Fig. 7 depicts the evolution of LA conversion and yield to DPA in a batch-mode experiment carried out for three days (72 h). As shown, over H-Beta 19 catalyst the reaction proceeds relatively fast, achieving already a high conversion within 6 h. It must be noted that for this transformation long reaction times (24–48 h) are usually presented in literature. The highest values were obtained after 72 h, leading to the outstanding catalytic performance of 77% $X_{LA}$, 70.2% $Y_{DPA}$, which means 91.2% of selectivity to diphenolic acid. Additionally, these values are especially remarkable considering the solvent less nature of the reaction media. Regarding the distribution of DPA isomers, the high shape selectivity towards *p,p′*-DPA isomer previously discussed for H-Beta 12.5 (Fig. 2) is kept in a similar level for H-Beta 19 as well.

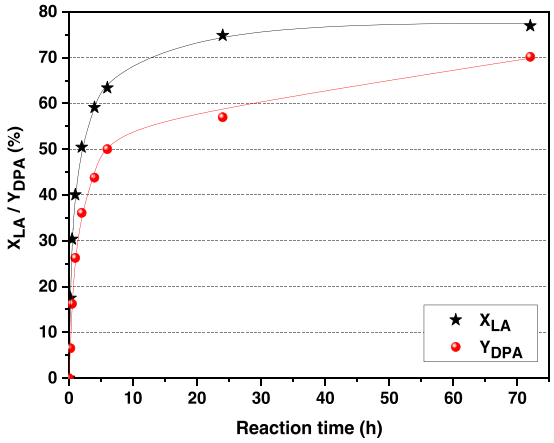


**Fig. 7.** Effect of reaction time on the solvent-free condensation of levulinic acid and phenol into diphenolic acid (DPA). Reaction conditions: 140 °C, 0.3 g catalyst loading, Phenol:LA = 6:1 (mol).

### 3.4. Reusability of H-Beta 19 catalyst

An evaluation of the stability in reaction of H-Beta 19 catalyst was performed under the optimized reaction conditions. Thus, a reutilization analysis was carried out, which consisted of three consecutive short reaction cycles (6 h, to avoid complete conversion conditions that would not allow for a proper discrimination of deactivation effects). After each reaction cycle, the catalyst was filtered, rinsed with acetone to remove remaining reaction media, and dried at RT overnight before the next use. Fig. 8 shows the results from this experiment in terms of conversion and yield, evidencing a progressive loss of the zeolite catalytic properties in each use. The decay is especially pronounced for the yield to DPA (from 50% to 28%), whereas the conversion of LA remains in higher values, implying a loss of selectivity to the desired product.

In order to determine the deactivation cause, wasted H-Beta 19 (after 3 uses) was analysed by thermogravimetric analysis to evaluate whether

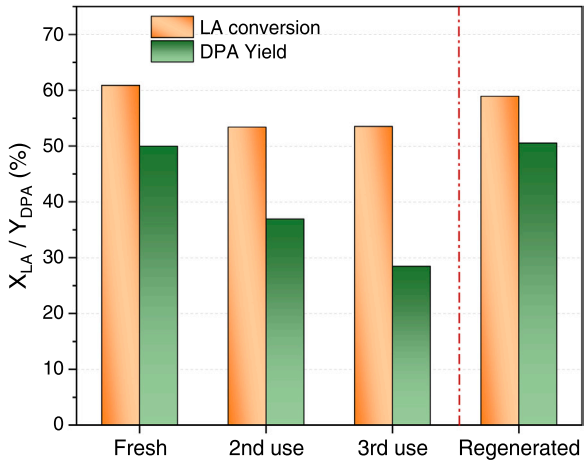


**Fig. 8.** Reusability of H-Beta 19 catalyst on the solvent-free condensation of levulinic acid and phenol into diphenolic acid (DPA). Reaction conditions: 140 °C, 0.30 g catalyst loading, 6 h, Phenol:LA = 6:1 (mol). Regeneration by calcination at 550 °C.

the deactivation comes from the formation of strongly adsorbed organic deposits on the acid sites of the material, since this is a typical cause of deactivation in lignocellulosic biomass-related catalytic processes. Fig. 9 depicts the TG analysis, confirming the presence of organic matter exothermally decomposing at 250–500 °C, accounting for approximately 10 wt% of the sample. Therefore, the formation of coke-like compounds on the strong acid sites of the zeolite, which hinders the progress of the catalytic reaction, is confirmed as the most plausible cause of deactivation. The catalyst was then regenerated by calcination in air (5 h at 550 °C) and used again in a fourth otherwise identical catalytic run. As shown in Fig. 8, the initial activity was recovered almost totally, especially in terms of yield to DPA. Therefore, the fouling of the catalyst surface is reversible by such thermal treatment, allowing for a longer operational life of the catalyst. As a conclusion, all together these results confirm that H-Beta 19 catalyst displays good reusability in the reaction.

## 4. Conclusions

Within this study, we have proved that readily accessible commercial acid zeolites are potential catalysts for the industrial production of DPA from levulinic acid and phenol. In particular, Beta zeolite with a moderate aluminum content (H-Beta 19, Si/Al=23) displays the best catalytic performance in the solvent-free condensation of LA and phenol, owing to the shape selectivity conferred by the BEA structure and to the adequate balance of acidity (Al content and speciation). Under the optimized reaction conditions (12 mmol LA, 140 °C, 0.30 g catalyst loading, Phenol:LA = 6:1 mol), over 70% yield to DPA with conversions of LA around 77% can be obtained after 72 h. Despite the catalyst showed a progressive loss of activity in successive uses, which is ascribed to a fouling effect by heavy organic deposits, the removal of such deposits by calcination in air allowed for a full recovery.

## CRediT authorship contribution statement

**Gabriel Morales:** Conceptualization, Funding acquisition, Writing – original draft preparation. **Juan A. Melero**: Supervision, Funding acquisition, Writing – review & editing. **Marta Paniagua**: Visualization, Investigation Writing – review & editing. **Clara López-Aguado**: Data curation. **Nora Vidal:** Methodology, Investigation.

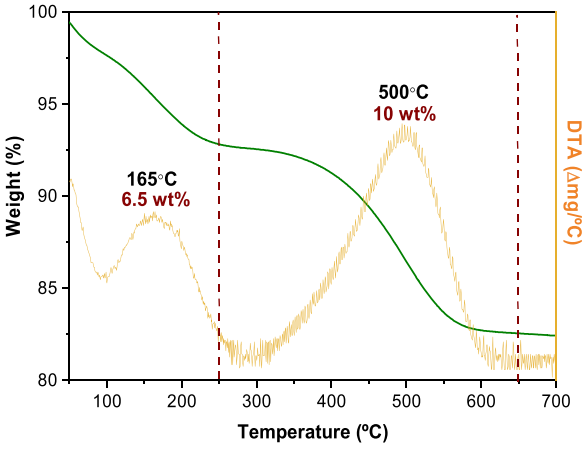


**Fig. 9.** TGA analysis of H-Beta 19 catalyst after three consecutive catalytic runs (recovered by filtration, rinsed with acetone and dried overnight). Reaction conditions: 140 °C, 0.30 g catalyst loading, 6 h, Phenol:LA = 6:1 (mol).

## Declaration of Competing Interest

The authors declare the following financial interests/personal relationships which may be considered as potential competing interests: Gabriel Morales reports financial support was provided by Spanish Ministry of Science and Innovation. Juan A. Melero reports financial support was provided by Regional Government of Madrid. Marta Paniagua reports financial support was provided by Regional Government of Madrid.

## Acknowledgements

The financial support by the projects RTI2018-094918-B-C42 (Spanish Ministry of Science and Innovation), S2018/EMT-4344 (Regional Government of Madrid), and M2181-BIOCAVI (Regional Government of Madrid and URJC), is gratefully acknowledged.

## References

[1] P.L. Arias, J.A. Cecilia, I. Gandarias, J. Iglesias, M. López Granados, R. Mariscal, G. Morales, R. Moreno-Tost, P. Maireles-Torres, Oxidation of lignocellulosic platform molecules to value-added chemicals using heterogeneous catalytic technologies, Catal. Sci. Technol. 10 (2020) 2721–2757, https://doi.org/10.1039/d0cy00240b.

[2] L. Wang, H. Wang, F. Liu, A. Zheng, J. Zhang, Q. Sun, J.P. Lewis, L. Zhu, X. Meng, F.S. Xiao, Selective catalytic production of 5-hydroxymethylfurfural from glucose by adjusting catalyst wettability, ChemSusChem 7 (2014) 402–406, https://doi.org/10.1002/cssc.201301076.

[3] B. Hu, K. Wang, L. Wu, S.H. Yu, M. Antonietti, M.M. Titirici, Engineering carbon materials from the hydrothermal carbonization process of biomass, Adv. Mater. 22 (2010) 813–828, https://doi.org/10.1002/adma.200902812.

[4] D. Mohan, C.U. Pittman, P.H. Steele, Pyrolysis of wood/biomass for bio-oil: a critical review, Energy Fuels 20 (2006) 848–889, https://doi.org/10.1021/ef0502397.

[5] D.M. Alonso, J.Q. Bond, J.A. Dumesic, Catalytic conversion of biomass to biofuels, Green Chem. 12 (2010) 1493–1513, https://doi.org/10.1039/c004654j.

[6] C.G.S. Lima, J.L. Monteiro, T. de Melo Lima, M. Weber Paixão, A.G. Corrêa, Angelica lactones: from biomass-derived platform chemicals to value-added products, ChemSusChem 11 (2018) 25–47, https://doi.org/10.1002/cssc.201701469.

[7] F. De Clippel, M. Dusselier, R. Van Rompaey, P. Vanelderen, J. Dijkmans, E. Makshina, L. Giebeler, S. Oswald, G.V. Baron, J.F.M. Denayer, P.P. Pescarmona, P.A. Jacobs, B.F. Sels, Fast and selective sugar conversion to alkyl lactate and lactic acid with bifunctional carbon-silica catalysts, J. Am. Chem. Soc. 134 (2012) 10089–10101, https://doi.org/10.1021/ja301678w.

[8] D.L. Klass, Biomass for renewable energy, fuels, and chemicals, Academic Press, 1998.

[9] G.W. Huber, S. Iborra, A. Corma, Synthesis of transportation fuels from biomass: chemistry, catalysts, and engineering, Chem. Rev. 106 (2006) 4044–4098, https://doi.org/10.1021/cr068360d.

[10] Z. Sun, B. Fridrich, A. De Santi, S. Elangovan, K. Barta, Bright side of lignin depolymerization: toward new platform chemicals, Chem. Rev. 118 (2018) 614–678, https://doi.org/10.1021/acs.chemrev.7b00588.

[11] T. Ennaert, J. Van Aelst, J. Dijkmans, R. De Clercq, W. Schutyser, M. Dusselier, D. Verboekend, B.F. Sels, Potential and challenges of zeolite chemistry in the catalytic conversion of biomass, Chem. Soc. Rev. 45 (2016) 584–611, https://doi.org/10.1039/c5cs00859j.

[12] Z. Zhang, J. Song, B. Han, Catalytic transformation of lignocellulose into chemicals and fuel products in ionic liquids, Chem. Rev. 117 (2017) 6834–6880, https://doi.org/10.1021/acs.chemrev.6b00457.

[13] D.P. Serrano, J.A. Melero, G. Morales, J. Iglesias, P. Pizarro, Progress in the design of zeolite catalysts for biomass conversion into biofuels and bio-based chemicals, Catal. Rev. Sci. Eng. 60 (2018) 1–70, https://doi.org/10.1080/01614940.2017.1389109.

[14] W. Schutyser, T. Renders, S. Van den Bosch, S.-F. Koelewijn, G.T. Beckham, B. F. Sels, Chemicals from lignin: an interplay of lignocellulose fractionation, depolymerisation, and upgrading, Chem. Soc. Rev. 47 (2018) 852–908, https://doi.org/10.1039/C7CS00566K.

[15] R. Rinaldi, R. Jastrzebski, M.T. Clough, J. Ralph, M. Kennema, P.C.A. Bruijnincx, B. M. Weckhuysen, Paving the way for lignin valorisation: recent advances in bioengineering, biorefining and catalysis, Angew. Chem. Int. Ed. 55 (2016) 8164–8215, https://doi.org/10.1002/anie.201510351.

[16] C. Chang, P. Cen, X. Ma, Levulinic acid production from wheat straw, Bioresour. Technol. 98 (2007) 1448–1453, https://doi.org/10.1016/j.biortech.2006.03.031.

[17] A. Mukherjee, M.J. Dumont, V. Raghavan, Review: sustainable production of hydroxymethylfurfural and levulinic acid: challenges and opportunities, Biomass Bioenergy 72 (2015) 143–183, https://doi.org/10.1016/j.biombioe.2014.11.007.

[18] Z. Fang, R.L. Smith, X. Qi, eds., Production of platform chemicals from sustainable resources, Springer Singapore, 2017. ⟨https://books.google.es/books?id=1zgoDwAAQBAJ&pg=PA46&lpg=PA46&dq=furfural+top-30&source=bl&ots=wsYAqSYBXz&sig=ACfU3U1HhLfoREFzpzVcbSO-flCp57UHww&hl=es&sa=X&ved=2ahUKEwjDvtDVsvrgAhVIUhoKHXNqAWIQ6AEwAXoECAkQAQ#v=onepage&q=furfural⟩ top-30&f=false (accessed March 11, 2019).

[19] M. Mascal, S. Dutta, L. Wu, Preparation of Compounds from Levulinic Acid, US 2018/0029980 A1,. ⟨http://www.freepatentsonline.com/20180029980.pdf⟩.

[20] F.D. Pileidis, M.M. Titirici, Levulinic acid biorefineries: new challenges for efficient utilization of biomass, ChemSusChem 9 (2016) 562–582, https://doi.org/10.1002/cssc.201501405.

[21] D.J. Hayes, S. Fitzpatrick, M.H.B. Hayes, J.R.H. Ross, The Biofine Process–Production of Levulinic Acid, Furfural, and Formic Acid from Lignocellulosic Feedstocks, in: Biorefineries-Industrial Processes and Products, Wiley-VCH Verlag GmbH, Weinheim, Germany, n.d.: pp. 139–164. https://doi.org/10.1002/9783527619849.ch7.

[22] G. Morales, J.A. Melero, J. Iglesias, M. Paniagua, C. López-Aguado, From levulinic acid biorefineries to γ-valerolactone (GVL) using a bi-functional Zr-Al-Beta catalyst, React. Chem. Eng. 4 (2019) 1834–1843, https://doi.org/10.1039/c9re00117d.

[23] F.D. Pileidis, M.-M. Titirici, Levulinic acid biorefineries: new challenges for efficient utilization of biomass, ChemSusChem 9 (2016) 562–582, https://doi.org/10.1002/cssc.201501405.

[24] G.C. Hayes, C.R. Becer, Levulinic acid: a sustainable platform chemical for novel polymer architectures, Polym. Chem. 11 (2020) 4068–4077, https://doi.org/10.1039/d0py00705f.

[25] M. Hartweg, C.R. Becer, Levulinic acid as sustainable feedstock in polymer chemistry, in: H.N. Cheng, R.A. Gross, P.B. Smith (Eds.), Green Polymer Chemistry: New Products, Processes, and Applications, American Chemical Society, 2018, pp. 331–338, https://doi.org/10.1021/bk-2018-1310.ch020.

[26] Z. Xue, Q. Liu, J. Wang, T. Mu, Valorization of levulinic acid over non-noble metal catalysts: challenges and opportunities, Green Chem. 20 (2018) 4391–4408, https://doi.org/10.1039/c8gc02001a.

[27] T.J. Malu, K. Manikandan, K.K. Cheralathan, Levulinic acid-a potential keto acid for producing biofuels and chemicals, in: Biomass, Biofuels, Biochemicals: Recent Advances in Development of Platform Chemicals, Elsevier Inc., 2019: pp. 171–197. https://doi.org/10.1016/B978–0-444–64307-0.00006–8.

[28] A. Dell'Acqua, B.M. Stadler, S. Kirchhecker, S. Tin, J.G.De Vries, Scalable synthesis and polymerisation of a β-angelica lactone derived monomer, Green. Chem. 22 (2020) 5267–5273, https://doi.org/10.1039/d0gc00338g.

[29] B.M. Stadler, A. Brandt, A. Kux, H. Beck, J.G. de Vries, Properties of novel polyesters made from renewable 1,4-pentanediol, ChemSusChem 13 (2020) 556–563, https://doi.org/10.1002/cssc.201902988.

[30] K. Yan, C. Jarvis, J. Gu, Y. Yan, Production and catalytic transformation of levulinic acid: a platform for speciality chemicals and fuels, Renew. Sustain. Energy Rev. 51 (2015) 986–997, https://doi.org/10.1016/j.rser.2015.07.021.

[31] H.R. Kricheldorf, R. Hobzova, G. Schwarz, Cyclic hyperbranched polyesters derived from 4,4-bis(4′ -hydroxyphenyl)valeric acid, Polymer 44 (2003) 7361–7368, https://doi.org/10.1016/j.polymer.2003.09.041.

[32] C. Zúñiga, M.S. Larrechi, G. Lligadas, J.C. Ronda, M. Galià, V. Cádiz, Polybenzoxazines from renewable diphenolic acid, J. Polym. Sci. Part A Polym. Chem. 49 (2011) 1219–1227, https://doi.org/10.1002/pola.24541.

[33] J. Iglesias, I. Martínez-Salazar, P. Maireles-Torres, D. Martin Alonso, R. Mariscal, M. López Granados, Advances in catalytic routes for the production of carboxylic acids from biomass: a step forward for sustainable polymers, Chem. Soc. Rev. 49 (2020) 5704–5771, https://doi.org/10.1039/d0cs00177e.

[34] Y. Liu, Y. Zhang, Z. Fang, Design, synthesis, and application of novel flame retardants derived from biomass, BioResources 7 (2012) 4914–4925, https://doi.org/10.15376/biores.7.4.4914-4925.

[35] J.J. Bozell, L. Moens, D.C. Elliott, Y. Wang, G.G. Neuenscwander, S.W. Fitzpatrick, R.J. Bilski, J.L. Jarnefeld, Production of levulinic acid and use as a platform chemical for derived products, Resour. Conserv. Recycl. 28 (2000) 227–239, https://doi.org/10.1016/S0921-3449(99)00047-6.

[36] R. Zhang, J.A. Moore, Synthesis, characterization and properties of polycarbonate containing carboxyl side groups, Macromol. Symp. 199 (2003) 375–390, https://doi.org/10.1002/masy.200350932.

[37] H. Mehdi, V. Fábos, R. Tuba, A. Bodor, L.T. Mika, I.T. Horváth, Integration of homogeneous and heterogeneous catalytic processes for a multi-step conversion of biomass: From sucrose to levulinic acid, γ-valerolactone, 1,4-pentanediol, 2-methyl-tetrahydrofuran, and alkanes, Top. Catal. 48 (2008) 49–54, https://doi.org/10.1007/s11244-008-9047-6.

[38] S. Van de Vyver, J. Geboers, S. Helsen, F. Yu, J. Thomas, M. Smet, W. Dehaen, Thiol-promoted catalytic synthesis of diphenolic acid with sulfonated hyperbranched poly(arylene oxindole)s, Chem. Commun. 48 (2012) 3497–3499, https://doi.org/10.1039/c2cc30239j.

[39] L.D. Mthembu, D. Lokhat, N. Deenadayalu, Catalytic condensation of depithed sugarcane bagasse derived levulinic acid into diphenolic acid, BioResources 16 (2021) 2235–2248, https://doi.org/10.15376/biores.16.2.2235-2248.

[40] M.J. Climent, A. Corma, S. Iborra, Converting carbohydrates to bulk chemicals and fine chemicals over heterogeneous catalysts, Green Chem. 13 (2011) 520–540, https://doi.org/10.1039/c0gc00639d.

[41] Y. Guo, K. Li, J.H. Clark, The synthesis of diphenolic acid using the periodic mesoporous H3PW12O40-silica composite catalysed reaction of levulinic acid, Green Chem. 9 (2007) 839–884, https://doi.org/10.1039/b702739g.

[42] Y. Guo, K. Li, X. Yu, J.H. Clark, Mesoporous H3PW12O40-silica composite: Efficient and reusable solid acid catalyst for the synthesis of diphenolic acid from levulinic acid, Appl. Catal. B Environ. 81 (2008) 182–191, https://doi.org/10.1016/j.apcatb.2007.12.020.

[43] K. Li, J. Hu, W. Li, F. Ma, L. Xu, Y. Guo, Design of mesostructured H3PW12O40-silica materials with controllable ordered and disordered pore geometries and their application for the synthesis of diphenolic acid, J. Mater. Chem. 19 (2009) 8628–8638, https://doi.org/10.1039/b910416j.

[44] S. Van De Vyver, J. Thomas, J. Geboers, S. Keyzer, M. Smet, W. Dehaen, P. A. Jacobs, B.F. Sels, Catalytic production of levulinic acid from cellulose and other biomass-derived carbohydrates with sulfonated hyperbranched poly(arylene oxindole)s, Energy Environ. Sci. 4 (2011) 3601–3610, https://doi.org/10.1039/c1ee01418h.

[45] H.F. Liu, F.X. Zeng, L. Deng, B. Liao, H. Pang, Q.X. Guo, Brønsted acidic ionic liquids catalyze the high-yield production of diphenolic acid/esters from renewable levulinic acid, Green Chem. 15 (2013) 81–84, https://doi.org/10.1039/c2gc36630d.

[46] D. Margolese, J.A. Melero, S.C. Christiansen, B.F. Chmelka, G.D. Stucky, Direct syntheses of ordered SBA-15 mesoporous silica containing sulfonic acid groups, Chem. Mater. 12 (2000) 2448–2459, https://doi.org/10.1021/cm0010304.

[47] J.A. Melero, G.D. Stucky, R. van Grieken, G. Morales, Direct syntheses of ordered SBA-15 mesoporous materials containing arenesulfonic acid groups, J. Mater. Chem. 12 (2002) 1664–1670, https://doi.org/10.1039/b110598c.

[48] D. Zhao, J. Feng, Q. Huo, N. Melosh, G.H. Fredrickson, B.F. Chmelka, G.D. Stucky, Triblock copolymer syntheses of mesoporous silica with periodic 50 to 300 angstrom pores, Science 279 (1998) 548–552, https://doi.org/10.1126/science.279.5350.548.

[49] F. Martínez, G. Morales, A. Martín, R. van Grieken, Perfluorinated Nafion-modified SBA-15 materials for catalytic acylation of anisole, Appl. Catal. A Gen. 347 (2008) 169–178, https://doi.org/10.1016/j.apcata.2008.06.015.

[50] P. Juárez, C. López-Aguado, M. Paniagua, J.A. Melero, R. Mariscal, G. Morales, Self-condensation of levulinic acid into bio-jet fuel precursors over acid zeolites: Elucidating the role of nature, strength and density of acid sites, Appl. Catal. A Gen. 631 (2022), 118480, https://doi.org/10.1016/j.apcata.2022.118480.

[51] X. Yu, Y. Guo, K. Li, X. Yang, L. Xu, Y. Guo, J. Hu, Catalytic synthesis of diphenolic acid from levulinic acid over cesium partly substituted Wells-Dawson type heteropolyacid, J. Mol. Catal. A Chem. 290 (2008) 44–53, https://doi.org/10.1016/j.molcata.2008.04.023.